UC Davis

UC Davis Previously Published Works

Title

DNA polymerases δ and λ cooperate in repairing double-strand breaks by microhomology-mediated end-joining in Saccharomyces cerevisiae

Permalink

https://escholarship.org/uc/item/2vm6z0z4

Journal

Proceedings of the National Academy of Sciences of the United States of America, 112(50)

ISSN

0027-8424

Authors

Meyer, Damon
Fu, Becky Xu Hua
Heyer, Wolf-Dietrich

Publication Date

2015-12-15

DOI

10.1073/pnas.1507833112

Peer reviewed

eScholarship.org Powered by the California Digital Library
University of California

CrossMark click for updates

DNA polymerases δ and λ cooperate in repairing double-strand breaks by microhomology-mediated end-joining in *Saccharomyces cerevisiae*

Damon Meyer[a,1], Becky Xu Hua Fu[a,2], and Wolf-Dietrich Heyer[a,b,3]

[a]Department of Microbiology and Molecular Genetics, University of California, Davis, CA 95616-8665; and [b]Department of Molecular and Cellular Biology, University of California, Davis, CA 95616-8665

Edited by Richard D. Kolodner, Ludwig Institute for Cancer Research, La Jolla, CA, and approved October 30, 2015 (received for review April 22, 2015)

Maintenance of genome stability is carried out by a suite of DNA repair pathways that ensure the repair of damaged DNA and faithful replication of the genome. Of particular importance are the repair pathways, which respond to DNA double-strand breaks (DSBs), and how the efficiency of repair is influenced by sequence homology. In this study, we developed a genetic assay in diploid *Saccharomyces cerevisiae* cells to analyze DSBs requiring microhomologies for repair, known as microhomology-mediated end-joining (MMEJ). MMEJ repair efficiency increased concomitant with microhomology length and decreased upon introduction of mismatches. The central proteins in homologous recombination (HR), Rad52 and Rad51, suppressed MMEJ in this system, suggesting a competition between HR and MMEJ for the repair of a DSB. Importantly, we found that DNA polymerase delta (Pol δ) is critical for MMEJ, independent of microhomology length and base-pairing continuity. MMEJ recombinants showed evidence that Pol δ proofreading function is active during MMEJ-mediated DSB repair. Furthermore, mutations in Pol δ and DNA polymerase 4 (Pol λ), the DNA polymerase previously implicated in MMEJ, cause a synergistic decrease in MMEJ repair. Pol λ showed faster kinetics associating with MMEJ substrates following DSB induction than Pol δ. The association of Pol δ depended on *RAD1*, which encodes the flap endonuclease needed to cleave MMEJ intermediates before DNA synthesis. Moreover, Pol δ recruitment was diminished in cells lacking Pol λ. These data suggest cooperative involvement of both polymerases in MMEJ.

DNA repair | genome stability | translocation

DNA double-strand breaks (DSBs) are toxic lesions that can be repaired by two major pathways in eukaryotes: nonhomologous end-joining (NHEJ) and homologous recombination (HR) (1). Although HR repairs DSBs in a template-dependent, high-fidelity manner, NHEJ functions to ligate DSB ends together using no or very short (1–4 bp) homology. Recently, a new pathway was identified in eukaryotes, which uses microhomologies (MHs) to repair a DSB and does not require the central proteins used in HR (Rad51, Rad52) or NHEJ (Ku70–Ku80) (2–5). In mammalian cells, this pathway of repair is known as alternative end-joining (Alt-EJ) and is often but not always associated with MHs, whereas in budding yeast, the commensurate pathway, MH-mediated end-joining (MMEJ), will typically use 5–25 bp of MH (6, 7). These pathways are associated with genomic rearrangements, and cancer genomes show evidence of MH-mediated rearrangements (8–12). In addition, eukaryotic genomes contain many dispersed repetitive elements that can lead to genome rearrangements when recombination occurs between them (13–16). Therefore, controlling DSB repair in the human genome, which features a variety of repeats, is especially important given the fact that recombination between repetitive elements has been implicated in genomic instability associated with disease (17–20).

The original characterization of Alt-EJ in mammalian cells suggested it did not represent a significant DNA repair pathway and only operated in the absence of functional HR and NHEJ pathways. More recent analyses demonstrate a physiological role of Alt-EJ during DNA repair in the presence of active HR and NHEJ pathways (2, 12, 21, 22). Furthermore, examination of I-*Sce*I–induced translocation junctions in mammalian cells revealed the frequent presence of MHs (23, 24). NHEJ-deficient and p53-null mice develop pro–B-cell lymphomas, and nonreciprocal translocations characterized by small MHs are found at their break point junctions (25–28). Similarly, in human cancers, many translocation break point junctions contain MHs, suggesting a role for Alt-EJ in cancer development (29–31) and resistance to chemotherapy and genetic disease (32–36). Hence, the presence of many short repetitive sequences in the human genome is likely to increase rearrangements mediated by MHs following the creation of a DSB.

MMEJ is a distinct DSB repair pathway that operates in the presence of functional NHEJ and HR pathways (10, 37). The genetic requirements of MMEJ are being studied in the model eukaryote *Saccharomyces cerevisiae* and involve components traditionally considered specific to the NHEJ (Pol λ) and HR (Rad1–Rad10, Rad59, and Mre11–Rad50–Xrs2) pathways (4, 5, 10, 38). Although being clearly independent of the central NHEJ factor Ku70–Ku80 heterodimer (10, 37), the involvement of the key HR factor Rad52 in MMEJ remains uncertain. It has been reported that Rad52 is required for MMEJ repair (4, 10, 38), whereas in another assay system Rad52 suppresses MMEJ repair (37). More recently, it has been proposed that the replication

Significance

The human genome contains many segments of short repetitive DNA, known as microhomologies, which are potential sites for the types of rearrangements found in many different types of cancer. Therefore, understanding how microhomologies within DNA can initiate chromosome rearrangements and the genes involved in promoting this process is critical in understanding cancer development. We examined the repair efficiency of DNA containing microhomologies and found a positive correlation between microhomology length and quality with repair efficiency. Furthermore, our work directly implicates the major DNA replication and repair polymerase, DNA polymerase δ, in repair of DNA damage using microhomologies, which act in conjunction with DNA polymerase λ. Our data suggest a two-polymerase model for microhomology-mediated end-joining.

Author contributions: D.M. and W.-D.H. designed research; D.M. and B.X.H.F. performed research; D.M. and W.-D.H. analyzed data; and D.M. and W.-D.H. wrote the paper.

The authors declare no conflict of interest.

This article is a PNAS Direct Submission.

Freely available online through the PNAS open access option.

[1]Present address: College of Health Sciences, California Northstate University, Sacramento, CA 95826.

[2]Present address: Departments of Pathology and Genetics, Stanford University School of Medicine, Stanford, CA 94305-5101.

[3]To whom correspondence should be addressed. Email: wdheyer@ucdavis.edu.

This article contains supporting information online at www.pnas.org/lookup/suppl/doi:10.1073/pnas.1507833112/-/DCSupplemental.

protein A (RPA) regulates pathway choice between HR and MMEJ (37). In addition, several models have been proposed that identify specific pathways that may use MHs for the repair of DNA damage (39–41). Despite current advancements in our understanding of MMEJ, the precise involvement of DNA polymerases in supporting the repair of DSBs using MHs remains poorly understood. DNA polymerase λ (also called Pol4 in budding yeast) and its human homolog Pol λ are considered to be the primary candidates for the DNA polymerases working in NHEJ and MMEJ (4, 5, 42–46). Both genetic and biochemical evidence shows that Pol δ is recruited during HR to extend Rad51-dependent recombination intermediates (47–50). Recent analysis using *pol32* mutants (5, 10) implicated the Pol32 subunit of Pol δ in MMEJ. Pol32 and Pol31 were also identified as subunits of the DNA polymerase zeta complex (Pol ζ) (51, 52), but previous analysis showed no effect of *rev3* mutants in MMEJ (10). *REV3* encodes the catalytic subunit of Pol ζ. However, an involvement of Pol δ had not been demonstrated directly before, and it is possible that Pol32 could act in conjunction with yet another DNA polymerase.

Here, we report the development of a series of interchromosomal MMEJ assays in diploid *S. cerevisiae* to assess the mechanisms underlying the repair of DSBs using varying MHs. We focus on diploid cells, as they represent the natural state of budding yeast, which is a diplontic organism (53). The yeast mating-type switching system represents a mechanism to return haploid yeast as efficiently as possible to diploidy (54). Using a combination of genetic, molecular, and in vivo chromatin immunoprecipitation (ChIP) experiments, we provide compelling evidence for a direct involvement of Pol δ in coordinating with Pol λ in MMEJ in budding yeast.

Results

Development of an Interchromosomal MMEJ Assay with Varying MH Length and Quality in Diploid *S. cerevisiae*. To determine the role of DNA polymerases in MMEJ repair, we designed a genetic assay in diploid *S. cerevisiae*, which measures interchromosomal MMEJ frequency by using varying lengths of complete or incomplete MH shared between two truncated *his3* alleles, *his3-Δ3′* and *his3-Δ5′* (Fig. 1*A*). The *his3-Δ3′* allele, located at the *HIS3* locus on chromosome XV, and the *his3-Δ5′* allele, at the *LEU2* locus on chromosome III, share increasing amounts of complete (16 bp, 20 bp, or 25 bp) or incomplete (14-**2**-2 bp, 14-**2**-4 bp, or 14-**2**-9 bp) MHs (Fig. 1*B*). The chromosome XV homolog shares no homology to either *his3* allele containing *his3Δ200*, which lacks the entire *HIS3* ORF and ∼200 bp of flanking sequence. Adjacent to each truncated *his3* allele is an HO endonuclease recognition sequence allowing for the creation of DSBs upon expression of the galactose-inducible HO endonuclease at the *trp1* locus (55). In addition to the truncated *his3* alleles, the mating-type loci (*MATa*, *MATα*) on chromosome III (Fig. 1*A*) are targeted by HO endonuclease, resulting in DSBs, which are repaired by HR or NHEJ (54). To simulate an acute exposure to a DNA damaging agent, the expression of HO endonuclease, and thereby DSB formation, was limited to 4 h. The utilization of MHs for repair is measured as the frequency of histidine prototrophs, scored on medium lacking histidine, compared with cell growth on the nutrient-rich medium, YPD (Table 1). Following DSB formation, cell viability was determined for wild-type and several key genotypes using the 14-**2**-4 bp substrate to assess whether viability differences confound determination of MMEJ frequencies. Viability varied maximally only about twofold compared with wild type (Table S1) and does not affect the conclusions about repair frequencies.

The MMEJ frequency of diploid wild-type cells containing both complete and incomplete MHs of varying lengths showed a concomitant increase in MMEJ frequency with increasing MH length (Table 1 and Fig. 2*A*). Further analysis showed that changing only a few base pairs of shared homology can significantly affect the MMEJ frequency, suggesting that MMEJ repair is sensitive to alterations within the sequences of the substrates. This is supported by an observed decrease in the repair frequency

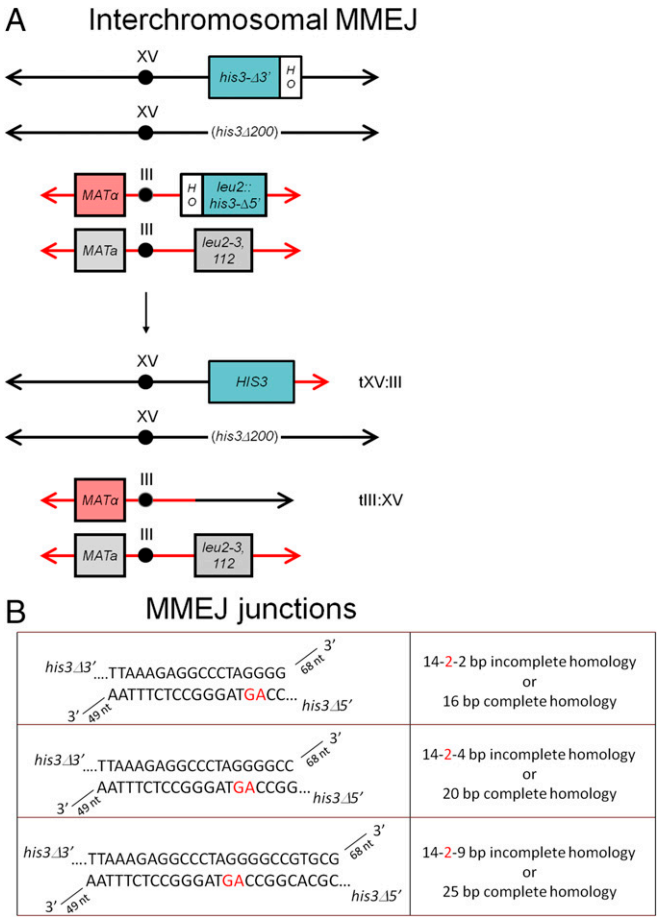

Fig. 1. Diploid MMEJ assays are defined by the length of MH and sequence continuity. (*A*) Recombination between *his3Δ3′* and *his3Δ5′* substrates on different chromosomes (interchromosomal MMEJ) generates *HIS3* recombinants measured by the number of histidine prototroph colonies on media lacking histidine. The homologous chromosome contains the *his3Δ200* allele, which is a complete deletion of the *HIS3* ORF. The 117 bp HO cut site (HO) is cut by a galactose-inducible HO endonuclease located at the *TRP1* locus (55). (*B*) The MMEJ junctions vary in homology length between the recombining *his3Δ3′* and *his3Δ5′* substrates from 16 to 25 bp and are fully complementary or contain a 2 bp mismatch (indicated in red) flanked by varying lengths of complementary sequences. The MMEJ junctions having incomplete homology are shown.

of the *his3-Δ3′* substrates containing a 2 bp mismatch (14-**2**-2 bp, 14-**2**-4 bp, and 14-**2**-9 bp) compared with the *his3-Δ3′* substrates having complete homology (16 bp, 20 bp, and 25 bp) in the shared MH with *his3-Δ5′* (Figs. 1*B* and 2*A*). These results are consistent with previous studies, which showed an increase in the length of MH leads to an increase in MMEJ frequency (4, 10, 37), whereas the presence of mismatches within the recombining MH decreases MMEJ repair frequency (4, 10). Furthermore, the proximity of the mismatch to the 3′-hydroxy end (14-**2**-2 bp, 14-**2**-4 bp, and 14-**2**-9 bp) results in a differential decrease in MMEJ repair of 153-fold, 21-fold, and 10-fold, respectively, compared with the complete homology substrates (Fig. 2*A*). These results demonstrate MMEJ occurs in diploid *S. cerevisiae* and is sensitive to the presence and location of sequence mismatches, in addition to the length of MH used for repair.

Analysis of wild-type unselected colonies grown on YPD and selected His^+ MMEJ recombinants following expression of the HO endonuclease revealed an intact *MATa*, *MATα*, and *leu2* locus for almost all of the colonies examined (Table S2). However, the presence of *his3-Δ3′* and *his3-Δ5′* was observed in only 8/16 and 7/16 unselected colonies tested, respectively. These results suggest that the repair of *MATa* and *MATα* occurs independent of

Table 1. Frequencies of interchomosomal MMEJ in wild-type and mutant diploid and haploid strains

Genotype*	14-**2**-2 bp	14-**2**-4 bp	14-**2**-9 bp	16 bp	20 bp	25 bp
Wild type	1.57×10^{-8} (1) [1.1–1.9]	4.51×10^{-7} (1) [3.5–5.0]	2.41×10^{-6} (1) [1.7–4.9]	1.2×10^{-6} (1) [0.53–2.0]	9.4×10^{-6} (1) [5.4–11.2]	2.7×10^{-5} (1) [0.9–5.5]
ku70Δ/ku70Δ	ND†	3.51×10^{-7} (↓1.2) [2.9–4.5]	ND	ND	5.1×10^{-6} (↓1.8) [1.4–11.2]	ND
rad52Δ/rad52Δ	1.8×10^{-6} (↑115) [1.2–2.2]	2.3×10^{-5} (↑51) [1.3–4.2]	1.5×10^{-4} (↑62) [1.1–1.9]	1.3×10^{-5} (↑10.8) [0.64–1.6]	7.3×10^{-5} (↑7.8) [5.5–8.9]	6.4×10^{-5} (↑24) [4.2–8.8]
rad51Δ/rad51Δ	1.1×10^{-6} (↑71) [0.8–1.4]	9.0×10^{-6} (↑20) [7.5–10.5]	ND	ND	8.0×10^{-5} (↑7.8) [4.9–9.1]	ND
rad1Δ/rad1Δ rad52Δ/rad52Δ	ND	1.1×10^{-6} (+2.4) [0.37–2.5]	ND	ND	ND	ND
pol4Δ/pol4Δ	ND	2.15×10^{-7} (↓2.1) [1.8–2.5]	ND	ND	ND	ND
dnl4Δ/dnl4Δ	1.0×10^{-8} (↓1.6) [5.3–1.2]	3.9×10^{-7} (↓1.2) [3.4–4.5]	ND	ND	5.8×10^{-6} (↓1.6) [4.7–7.5]	ND
pol4Δ/pol4Δ rad52Δ/rad52Δ	ND	6.0×10^{-6} (+13.3) [4.4–7.3]	ND	ND	ND	ND
pol4Δ/pol4Δ pol32Δ/pol32Δ	ND	1.7×10^{-10} (↓2441) [0.8–2.1]	ND	ND	ND	ND
pol4Δ/pol4Δ pol3-ct/pol3-ct	ND	1.3×10^{-10} (↓3192) [1.0–3.3]	ND	ND	ND	ND
pol32Δ/pol32Δ	3.8×10^{-9} (↓4.2) [2.1–6.3]	5.2×10^{-8} (↓8.3) [2.1–6.9]	5.1×10^{-8} (↓50) [3.3–10.5]	ND	5.5×10^{-8} (↓167) [1.4–9.6]	ND
pol3-ct/pol3-ct	1.0×10^{-9} (↓15.6) [0.6–2.3]	2.6×10^{-9} (↓167) [1.9–3.6]	3.0×10^{-7} (↓8.3) [1.7–4.4]	ND	1.2×10^{-6} (↓7.7) [0.8–2.1]	ND
rev3Δ/rev3Δ	1.2×10^{-8} (↓1.2) [1.0–3.0]	2.4×10^{-7} (↓1.9) [1.4–3.4]	1.2×10^{-6} (↓2) [0.6–1.6]	ND	8.6×10^{-6} (↓1.1) [4.7–11.9]	ND
pol4Δ/pol4Δ rev3Δ/rev3Δ	ND	1.4×10^{-7} (↓3.2) [0.9–2.0]	1.5×10^{-6} (↓1.6) [0.7–2.0]	ND	ND	ND
pol3-01/pol3-01	3.7×10^{-9} (↓4.2) [2.5–6.0]	1.55×10^{-7} (↓2.9) [1.2–2.7]	1.7×10^{-6} (↓1.4) [0.8–2.5]	ND	ND	ND
msh2Δ/msh2Δ	ND	1.2×10^{-7} (↓3.8) [0.8–1.8]	ND	ND	3.2×10^{-6} (↓2.9) [1.4–4.9]	ND
rad59Δ/rad59Δ	ND	1.4×10^{-7} (↓3.2) [0.5–2.3]	ND	ND	4.2×10^{-6} (↓2.2) [1.3–6.5]	ND
rad59Δ/rad59Δ rad52Δ/rad52Δ	ND	7.4×10^{-6} (+16.4) [5.0–8.4]	ND	ND	ND	ND
Wild type‡ *Mata-inc* (Haploid)	ND	1.93×10^{-7} (1) [1.3–3.2]	ND	ND	ND	ND
Wild type‡ *Matα* (Haploid)	ND	1.57×10^{-7} (↓1.2) [0.9–2.8]	ND	ND	ND	ND
rad52Δ‡ Mata-inc (Haploid)	ND	2.3×10^{-6} (11.9) [1.2–4.0]	ND	ND	ND	ND
rad52Δ‡ *Matα* (Haploid)	ND	1.51×10^{-6} (7.8) [1.1–2.2]	ND	ND	ND	ND

The median translocation frequency was determined for each strain from at least 15 independent cultures. Fold increase (↑) or decrease (↓), rounded to integers, from the median frequency obtained with the wild-type strain, is indicated in parentheses. The 95% confidence intervals were determined using Table S5 and are indicated in brackets.

*All strains possess the *his3-Δ5′* substrate at the *LEU2* locus on one copy of chromosome III and the *his3-Δ3′* substrate at the *HIS3* locus (Fig. 1). The *his3-Δ5′* and *his3-Δ3′* substrates share varying MHs of *HIS3* coding sequence indicated above each column. Complete genotypes are given in Table S3.

†Frequency not determined (ND).

‡Haploid strains.

MMEJ. The loss of *his3-Δ3′* and *his3-Δ5′* is consistent with repair by HR using the homolog as a template. Furthermore, an intact *leu2* locus demonstrates at least one chromosome III homolog is recovered following DSB induction. Identification of the reciprocal translocation (see Fig. 1*A*) occurred only in a small subset of His^+ recombinants (1/14), which is similar to previous reports (55, 56) (Table S2).

MMEJ Is Independent of Ku70 and Ligase 4 but Suppressed by Rad52. To ascertain whether our assay fulfills the criteria that define MMEJ, we examined the effect of *ku70Δ*, *lig4Δ*, and *rad52Δ* single mutants on the frequency of MMEJ repair. Because MMEJ in budding yeast was initially defined as being independent of Ku70, Ligase 4, and Rad52 (5, 10), we expected the loss of either Ku70 Ligase 4 or Rad52 function to have little effect on the overall frequency of MMEJ repair. However, recent findings have shown MMEJ requires or is inhibited by Rad52 depending on the length of MH (4, 10, 37, 38). Using the intermediate MMEJ substrates (14-**2**-4 bp and 20 bp), we observed no significant difference in MMEJ repair frequency between *ku70Δ/ku70Δ* or *lig4Δ/lig4Δ* mutants and wild-type cells (Fig. 2*B* and Table 1). In contrast, the *rad52Δ/rad52Δ* mutants showed a dramatic increase in MMEJ repair frequency for both substrates tested (Fig. 2*B* and Table 1), suggesting Rad52 can inhibit DSB repair using MHs. We confirmed

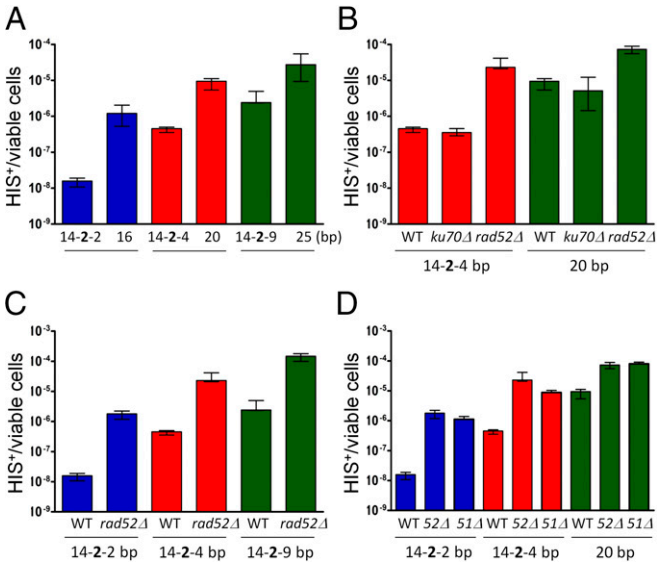

Fig. 2. MMEJ is influenced by Rad52, Rad51, the length and continuity of MH, but is independent of Ku70. (*A–D*) The median frequency, ±95% confidence interval, of interchromosomal MMEJ between the *his3Δ3′* and *his3Δ5′* substrates was calculated from a minimum of 20 independent cultures. Homology shared between *his3Δ3′* and *his3Δ5′* varies in length and the presence (14-**2**-2, 14-**2**-4, or 14-**2**-9 bp) or absence (16, 20, or 25 bp) of a 2 bp mismatch. All strains are diploid and homozygous for the indicated mutation. (*A*) Analysis of MMEJ frequencies in wild-type (WT) strains containing MH of 14-**2**-2 (WDHY2948), 16 (WDHY3427), 14-**2**-4 (WDHY2949), 20 (WDHY3188), 14-**2**-9 (WDHY3001), and 25 bp (WDHY3426). (*B*) MMEJ frequencies of *ku70Δ* (WDHY3281 and WDHY4391) or *rad52Δ* (WDHY3475 and WDHY3598) single mutants in the MMEJ assay with (14-**2**-4 bp) or without (20 bp) a 2 bp mismatch within the MH. (*C* and *D*) Influence of *rad52Δ* (WDHY3644, WDHY3475, and WDHY3597) single mutants (*C*) and *rad51Δ* (WDHY4352, WDHY4423, and WDHY4502) single mutants (*D*) in the MMEJ assay containing varying lengths of homology. The *rad52Δ* single mutant MMEJ frequencies using 14-**2**-2, 14-**2**-4, or 20 bp of MH are represented in panels *C* and *D*, *B–D*, and *B* and *D*, respectively.

this inhibitory effect of Rad52 using other MMEJ substrate variants, which are independent of MH length, sequence continuity, and cell viability (Fig. 2*C*, Table 1, and Table S1). In addition, unselected colonies and His^+ recombinants from *rad52Δ* mutants retained at least one chromosome III homolog, but only 12/18 YPD colonies retained both *MATα* and *his3Δ5′* located on either side of the chromosome III centromere (Table S2; see Fig. 1*A*). This suggests that two simultaneous breaks on chromosome III in *rad52Δ* mutants lead to increased chromosome loss. Rad52 has several functions in DSB repair, which include annealing of single-stranded homologous sequences or the replacement of RPA-coated single-strand DNA with Rad51 to form a nucleoprotein filament required for HR. To determine if the inhibitory effect observed in *rad52Δ* mutants is due to Rad51 filament formation, we examined *rad51Δ*/*rad51Δ* mutants. MMEJ frequencies were very similar in the *rad51Δ* and *rad52Δ* mutants (Fig. 2*D* and Table 1), suggesting HR directly competes with MMEJ in DSB repair through the formation of Rad51 nucleoprotein filaments mediated by Rad52.

To test if HR competes with MMEJ through the formation of Rad51 nucleoprotein filaments and the subsequent repair using the homologous chromosome, we analyzed MMEJ repair in wild-type and *rad52Δ* mutants in haploid strains possessing the 14-**2**-4 bp substrate. Under these conditions, haploid wild-type cells showed a small, but significant, decrease in MMEJ repair frequency compared with diploid wild-type cells. This effect is independent of DSB formation at the *MAT* locus and is not accompanied by a significant drop in cell viability (Table 1 and Table S1). However, haploid *rad52Δ* mutants display a smaller increase in MMEJ repair frequency than diploid *rad52Δ* mutants compared with haploid or diploid wild-type cells, respectively. Again, this effect is not due to decreased cell viability or DSB formation at the *MAT* locus (Table 1 and Table S1). These results suggest Rad52 functions to inhibit MMEJ by promoting Rad51 filament formation and thereby HR but does not require the presence of a homologous template.

DNA Polymerase δ Promotes MMEJ Repair. The major emphasis of previous studies analyzing the genetic requirements of MMEJ has focused on components predicted to function in the early steps of resection, annealing, and end-processing of the nonhomologous 3′ flap (4, 5). However, only a few of these studies have examined the role of DNA polymerases in the final steps of MMEJ repair. Although a role for Pol λ in MMEJ has been previously reported (4, 5), an involvement of other DNA polymerases is unclear in *S. cerevisiae*. A recent report demonstrated a role of the nonessential DNA polymerase subunit Pol32 in MMEJ (10). Pol32 associates with Pol31 and the catalytic subunit Pol3 to form the hetero-trimeric DNA polymerase delta (Pol δ), which functions in lagging strand synthesis during DNA replication and in the extension of HR intermediates (47, 48, 50, 57–59). In addition, DNA polymerase ζ (Pol ζ) is composed of the Rev3–Rev7 heterodimer and functions in DNA translesion synthesis as a four-subunit Pol ζ complex with Pol32 and Pol31 (51, 52). Therefore, the involvement of Pol32 in MMEJ repair suggests that either Pol δ or Pol ζ, or both, is potentially involved in the repair of DSBs using MHs during the extension step of MMEJ. To examine the role of Pol32 further, we tested *pol32Δ*/*pol32Δ* mutants in our diploid MMEJ assay and found a significant decrease in the frequency of MMEJ repair compared with wild type regardless of MH length or the presence of a mismatch (Fig. 3*A* and Table 1). Depending on the specific substrate, 76% to ≥99% of the recombinants depended on Pol32 (Table 1). Because this decrease in *pol32Δ* mutants could be due to its interaction with Pol ζ, we decided to test the effect of the *rev3Δ* mutation on MMEJ repair to determine if a similar decrease was also observed. A modest decrease of twofold was observed in *rev3Δ*/*rev3Δ* mutants using the 14-**2**-4 bp and 14-**2**-9 bp MH substrates for MMEJ repair, whereas the 14-**2**-2 bp and 20 bp MH substrates showed no defect in MMEJ repair (Table 1). Instead, the *pol32*Δ mutation exerted its largest effect on the 20 bp MH substrate (Table 1), demonstrating that Pol32 and Rev3 show different substrate specificity. Taken together, these results demonstrate a robust and consistent role of Pol32 in promoting MMEJ repair, which is mainly independent of Rev3 function.

The above results suggest the defect observed in *pol32Δ*/*pol32Δ* cells is through its interaction with Pol3 and Pol31 in forming Pol δ. The involvement of Pol δ in MMEJ is more difficult to test directly, as both *POL31* and *POL3* are essential genes. However, there are several alleles of *POL3*, which alter the protein function but allow for cell growth. One such allele is *pol3-ct*, which is missing the last four C-terminal amino acids and was originally identified as a mutant defective in meiotic gene conversion (60). Subsequent analysis revealed that in addition to its meiotic phenotypes, *pol3-ct* was also defective in mitotic gene conversion and break-induced replication (BIR) due to a decrease in the interaction between Pol3 and Pol31 resulting in an unstable Pol δ complex (48, 61, 62). To determine if the role of Pol32 in MMEJ repair was due to a defect in the Pol δ complex, we tested the frequency of MMEJ in *pol3-ct*/*pol3-ct* mutants. A significant decrease in the frequency of MMEJ was observed in *pol3-ct*/*pol3-ct*, which was similar to the *pol32Δ*/*pol32Δ* mutants (Fig. 3*B* and Table 1). The cell viability of *pol3-ct* and *pol32Δ* mutants is similar to wild type and each other (Table S1). These results show the involvement of Pol32 in MMEJ is due to the action of Pol δ in promoting the repair of DSBs using MHs and is

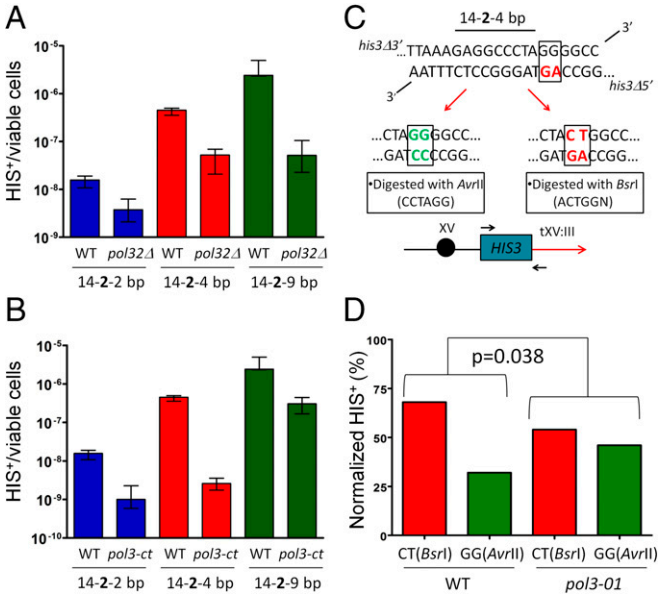

Fig. 3. DNA polymerase δ promotes MMEJ independent of MH length and can correct mismatched nucleotides near the 3′-hydroxyl end. (*A* and *B*) The median frequency, ±95% confidence interval, of interchromosomal MMEJ between the *his3Δ3′* and *his3Δ5′* substrates was calculated from a minimum of 20 independent cultures. Homology shared between *his3Δ3′* and *his3Δ5′* varies in length (14-**2**-2, 14-**2**-4, or 14-**2**-9 bp) and contains a 2 bp mismatch. The contribution of Pol32 (WDHY4390, WDHY3126, and WDHY3165) (*A*) and the DNA polymerase δ allele, *pol3-ct* (WDHY3872, WDHY3809, WDHY3810, and WDHY3807) (*B*), in promoting MMEJ using varying lengths of MH compared with wild-type (WT) (WDHY2948, WDHY2949, and WDHY3001). (*C* and *D*) Sequence analysis of histidine prototrophic colonies following MMEJ repair in WT (WDHY2949) and cells harboring the exonuclease-defective DNA polymerase δ allele, *pol3-01* (WDHY3809 and WDHY3807). Correction of the 2 bp GG mismatch on the top strand would result in a CT conversion, thereby making the sequence sensitive to *Bsr*I digestion. Retention of the 2 bp GG mismatch on the top strand would allow for digestion with *Avr*II. Initially 20 colonies were chosen for genomic DNA extraction, PCR amplification of the His$^+$ recombinant (using primers indicated as arrows in *C*), digestion with both *Avr*II and *Bsr*I, and then verification by sequencing. Subsequent His$^+$ recombinants were collected as above but were digested with both *Avr*II and *Bsr*I to determine sequence and not sent for sequencing. A total of 121 WT and 100 *pol3-01* His$^+$ recombinants were analyzed, and the two sets of data were compared using a contingency table and Fisher's exact test.

the first direct evidence, to our knowledge, demonstrating the involvement of Pol δ in MMEJ repair. Although the overall quantitative effect of the *pol32Δ* and *pol3-ct* mutation was similar, the substrate specificity pattern is somewhat different between both. Although *pol32*Δ mutants had the largest effect on the 20 bp MH substrate, the *pol3-ct* mutation affected the 14-**2**-4 bp substrate most. This suggests greater complexity and potential for the involvement of multiple DNA polymerases in a single MMEJ event.

To further investigate the role of Pol δ in MMEJ repair, we analyzed the junction sequence of His$^+$ recombinants from cells, which used 14-**2**-4 bp of shared MH between the *his3-Δ3′* and *his3-Δ5′* alleles for repair (Fig. 3*C*). The exonuclease activity of Pol δ has been shown to be active during DSB repair (40, 63). We chose the 14-**2**-4 bp substrate to be within the range of the Pol δ proofreading window (64). The 2 bp mismatch, which exists between the *his3-Δ3′* and *his3-Δ5′* alleles, can be corrected by mismatch repair, resulting in two distinct classes of His$^+$ recombinants in equal proportions that can be distinguished by restriction digestion using either *Avr*II or *Bsr*I (Fig. 3*C*). Alternatively, the two mismatched guanine nucleotides on *his3-Δ3′* located close to the 3′-hydroxyl end could be corrected by the proofreading exonuclease activity of Pol δ, which would bias the outcome toward His$^+$ recombinants digested by the *Bsr*I restriction enzyme. In fact, 82 out of 121 (68%) of all His$^+$ recombinants recovered from wild-type cells were digested by *Bsr*I, demonstrating a significant bias toward one class of MMEJ recombinants, which is potentially mediated by the exonuclease function of Pol δ (Fig. 3*D*). This is in contrast to His$^+$ recombinants from cells using the 14-**2**-2 bp or 14-**2**-9 bp substrates for repair, which showed 20 out of 20 and 12 out of 32 were digested by *Bsr*I, respectively. To test if the exonuclease function of Pol δ biased the His$^+$ recombinants toward the *Bsr*I class, we examined 100 independent His$^+$ recombinants from cells containing the 14–**2**-4 bp substrate in the exonuclease-defective *pol3-01* strain (65). The *Avr*II and *Bsr*I classes of His$^+$ recombinants recovered from *pol3-01/pol3-01* were in near equal proportion and significantly different from wild type (P value = 0.0385; Fig. 3*D*). All His$^+$ recombinant junctions were susceptible to either *Avr*II or *Bsr*I, showing that all products underwent faithful repair. These results provide further independent evidence for a role of Pol δ in the extension of intermediates during MMEJ repair.

DNA Polymerase δ Associates with DSBs During MMEJ Repair. Because the results of our genetic experiments demonstrate that Pol δ is involved in MMEJ repair, we decided to investigate the physical association of Pol3 with the *his3-Δ3′* MMEJ substrate before and after DSB formation using ChIP (Fig. 4*A*). These experiments were performed in *rad52Δ/rad52Δ* strains that contained the 14-**2**-4 bp of shared MH between the *his3-Δ3′* and *his3-Δ5′* alleles, allowing for an increased probability of cross-linking Pol3 to the MMEJ substrate due to the higher frequency of repair. Following the addition of galactose to the cell cultures, a progressive increase in DSB formation was observed, which peaked at 90% after 2 and 4 h of HO endonuclease induction (Fig. 4*C*), consistent with previous analyses (66). The kinetics of Pol3 recruitment at *his3-Δ3′* follows DSB formation, with an apparent 2 h delay, showing a 3.5-fold and sixfold enrichment of *his3-Δ3′* Pol3 ChIP over background at the 2 and 4 h time points, respectively (Fig. 4*C*). To simulate the genetic MMEJ assay, cells were collected, washed, and placed in YPD after 4 h to repress HO endonuclease expression and continue growth. Following this shift to YPD, we saw a decrease in the presence of the DSB from 6 to 12 h, which is a measure of cells rejoining the broken chromosome ends by NHEJ and subsequent growth of those cells within the culture over the indicated time course (Fig. 4*C*). In contrast, the 11-fold and fourfold enrichment of *his3-Δ3′* at 6 and 8 h, respectively, demonstrates that Pol3 is functioning in MMEJ after DSB formation (Fig. 4*C*). By 12 h, there is no detectable enrichment of *his3-Δ3′*, indicating the repair process is completed by this time (Fig. 4*C*). Taken together, these results provide direct evidence for the involvement of Pol3, and thereby Pol δ, in the repair of DSBs using MHs.

The involvement of Pol δ in extending MMEJ repair intermediates suggests its role is dependent on the activities of proteins that function to process the DSBs before extension. Resection of the DSBs and annealing using MHs are required to form an intermediate containing 3′ heterologous flaps derived from HO endonuclease cutting of the 117 bp HO endonuclease recognition sequence (Fig. 1*B*). The removal of these 3′ heterologous flaps requires the action of the Rad1–Rad10 endonuclease (67) and should be necessary for Pol δ extension. Therefore, *rad1* mutants should diminish the association of Pol δ with the MMEJ recombination intermediate and reduce the overall repair efficiency. To test this, we repeated the above ChIP experiments with *rad1Δ/rad1Δ rad52Δ/rad52Δ* double mutants and examined the association of Pol3 with *his3-Δ3′* over the indicated time course (Fig. 4*C*). The absence of Rad1 results in a significant decrease in the association of Pol3 with *his3-Δ3′* from 2 to 8 h compared with cells containing Rad1 (Fig. 4*C*), which correlates

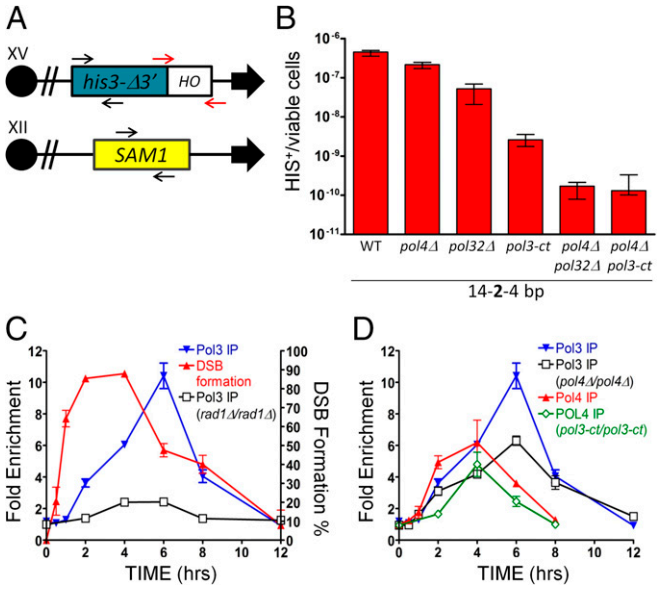

Fig. 4. DNA polymerases δ and λ associate with a DSB containing MHs and cooperate in the subsequent repair of a DSB using MMEJ. (*A*) Diagram of the chromosomal loci and the relative location of primers used in the quantification of DSB formation (red arrows) or ChIP analysis (black arrows) of DNA polymerase δ and λ. (*B*) The median frequency, ±95% confidence interval, of *pol4Δ*, *pol32Δ*, *pol3-ct*, *pol4Δ pol32Δ*, and *pol4Δ pol3-ct* single and double mutants using 14-**2**-4 bp of MH between the *his3Δ3′* and *his3Δ5′* substrates was calculated from a minimum of 20 independent cultures. The *pol32Δ* and *pol3-ct* single mutants are also represented in Fig. 3 *A* and *B*, respectively. (*C*) DSB formation was analyzed using qPCR by comparing the formation of a PCR product using primers flanking the HO endonuclease recognition cut site (red arrows in *A*) relative to the PCR product of *SAM1* (black arrows in *A*), before and after HO endonuclease induction over the indicated time course (red triangle). DNA following ChIP, using antibodies to Pol3, was analyzed using qPCR by comparing the PCR product from *his3Δ3′* to *SAM1* (black arrows in *A*) both before and after DSB induction over the indicated time course (Pol3 IP, *rad52Δ/rad52Δ*, blue triangle; *rad1Δ/rad1Δ rad52Δ/rad52Δ*, black square). The mean ± SEM of samples taken at the indicated time points from two independent cultures (WDHY3475, WDHY4487), grown concurrently, is represented. The Pol3 IPs in *rad52Δ/rad52Δ* (blue triangle) strains are represented in *C* and *D*. (*D*) ChIP analysis as in *C* using antibodies to Pol3 or Pol λ as indicated (Pol3 IP, *rad52Δ/rad52Δ*, blue triangle; Pol3 IP, *pol4Δ/pol4Δ rad52Δ/rad52Δ*, black square; Pol λ IP, *rad52Δ/rad52Δ*, red triangle; Pol λ IP, *pol3-ct/pol3-ct rad52Δ/rad52Δ*, green diamond). The mean ± SEM of samples taken at the indicated time points from two independent cultures (WDHY3475 and WDHY3793), grown concurrently, is represented.

with a 21-fold decrease in the frequency of His^+ recombinants compared with *rad52Δ/rad52Δ* (Table 1). These results demonstrate a strong genetic dependence of MMEJ on the heterologous flap cleavage activity of Rad1–Rad10 as a prerequisite for extension by Pol δ.

DNA Polymerases δ and λ Cooperate to Repair DSBs Using MMEJ. Studies on MMEJ using shorter MHs of 8–12 bp have implicated the involvement of Pol λ (4, 5), but longer MHs were not examined. Therefore, we tested *pol4Δ/pol4Δ* mutants in the MMEJ repair assay using 14-**2**-4 bp of MH and observed a twofold decrease in the frequency of MMEJ while maintaining cell viability similar to wild type (Fig. 4*B*, Table 1, and Table S1). The involvement of Pol4 in NHEJ prompted the examination of *pol4Δ* mutants for intact *MATa*, *MATα*, *leu2-3,112*, *his3Δ3′*, and *his3Δ5′* loci in unselected and His^+ recombinant colonies. A similar proportion of intact *MATa*, *MATα*, and *leu2* loci in unselected and His+ recombinant colonies was observed in wild-type and *pol4Δ* mutants (Table S2). However, a noticeable decrease of intact *his3Δ3′* and *his3Δ5′* loci in *pol4Δ* mutants suggests a defect in NHEJ, resulting in a higher use of HR in repair using the homologous chromosome (Table S2).

Next, the interaction between Pol λ and Pol δ in MMEJ was determined through epistasis analysis of *pol4Δ/pol4Δ pol32Δ/pol32Δ* and *pol4Δ/pol4Δ pol3-ct/pol3-ct* double mutants using 14-**2**-4 bp of MH for repair. A similar synergistic decrease in MMEJ frequency of over 2,500-fold was observed in both double mutants and is not due to a decrease in cell viability (Fig. 4*B*, Table 1, and Table S1). This suggests that Pol λ and Pol δ cooperate in MMEJ. To exclude the possibility of Pol32 exerting its effect with Pol4 as part of the Pol ζ complex, the MMEJ frequency of *pol4Δ/pol4Δ rev3Δ/rev3Δ* double mutants was tested and showed no significant decrease from single *pol4Δ* mutants (Table 1).

To provide additional evidence that Pol λ is functioning in MMEJ, we tested its physical association with the *his3-Δ3′* MMEJ substrate using ChIP, as performed above with Pol3. We observed a fivefold and sixfold enrichment of *his3-Δ3′* over background at the 2 and 4 h time points, respectively (Fig. 4*D*). The above enrichment is specific, as the *pol4Δ/pol4Δ rad52Δ/rad52Δ* double mutants show no significant enrichment of *his3-Δ3′* above background for the 2 and 4 h time points. However, unlike Pol3, enrichment of Pol λ peaked at 6 h and decreased to 3.5-fold at 6 h and was indistinguishable from background at 8 h (Fig. 4*D*), suggesting a possible earlier role for Pol λ than Pol δ in MMEJ. Finally, recruitment of Pol3 and Pol4 to the DSB was interdependent (Fig. 4*D*), consistent with a two-polymerase model for MMEJ-mediated DSB repair.

Discussion

Here, we developed an interchromosomal MMEJ repair assay in diploid *S. cerevisiae* to assess the repair of simultaneous DSBs using MHs of varying lengths and sequence continuity. The study of MMEJ in diploids represents a departure from previously published reports (5, 10, 37) in haploid budding yeast and was chosen because it is the natural state of *S. cerevisiae* (53). Although NHEJ is suppressed in diploids (68–70), we find the broken loci at *MATa*, *MATα*, *his3Δ3′*, and *his3Δ3′* are often repaired by HR or NHEJ potentially due to acute HO endonuclease induction, which results in similar cell viability in many mutants tested compared with wild type. Similar to the results of Villarreal et al. with haploid yeast cells and shorter MHs of 6–18 bp, we find a correlation between increasing MH length and MMEJ repair in wild-type cells with MHs of 16–25 bp (10). Using the *his3* MMEJ substrates in haploid yeast yields a significantly lower repair frequency, possibly due to the requirement of the reciprocal translocation in MMEJ His^+ recombinants for viability. In addition, the presence of a di-nucleotide mismatch significantly decreased the frequency of MMEJ. The most dramatic decrease of nearly 100-fold was observed when using the 14-**2**-2 bp MH substrate for repair, indicating that the nearer the dinucleotide mismatch was to the 3′-hydroxyl end of the MH, the greater its repressive effect on MMEJ repair. This suggests that the mismatch had a destabilizing effect on the MH pairing intermediate and/or the subsequent extension of the 3′-hydroxyl end by a DNA polymerase. This effect is potentially due to the proximity of the mismatch to the 3′-hydroxyl end, which could destabilize the terminal base pairing, resulting in only 14 bp of MH used for repair. Hence, the length and degree of mismatching of the MH have a major impact on the efficiency of repair, which is possibly mediated by the thermostability of the MH pairing intermediate.

The role of Rad52 in MMEJ repair has been unclear, as initial studies suggested MMEJ was independent of Rad52 (3). In contrast to more current reports, which show the use of longer MHs (≥15 bp) for repair is Rad52-dependent, while Rad52 is inhibitory when short MHs are used for repair (≤14 bp) (10, 37). In our system, we observed an inhibitory effect of Rad52 on the frequency of MMEJ repair regardless of homology length, similar to other published observations (37). This is in contrast to Villarreal et al., who saw a dependence on Rad52 for MMEJ repair using MHs ≥15 bp but an inhibitory effect of Rad52 when MHs used to repair

the DSB were ≤13 bp (10). These disparate results could be the consequence of differences in the experimental design (acute vs. chronic, DSB formation), the presence of longer nonhomologous flaps, and the effect of ploidy on MMEJ. Rad52 functions to promote HR by loading Rad51 on RPA-coated ssDNA to form a Rad51 nucleoprotein filament that searches the genome for homologous sequences (71). In addition, Rad52 efficiently anneals protein-free and RPA-coated ssDNA (72, 73). One possible mechanism for an inhibitory effect of Rad52 on MMEJ could be through the loading of Rad51 and subsequent allelic recombination after extensive resection on either side of the DSB to reveal homologous sequences for recombination, thereby generating a histidine auxotroph. This is supported by a similar inhibitory effect of *rad51Δ* and *rad52Δ* mutants on MMEJ frequency, indicating there is little if any inhibitory role of Rad52 on MMEJ, which is independent of Rad51. In addition, Rad59 has been shown in diploids to function in single-strand annealing (SSA) independent of Rad52 (55), and we observe a differential effect of *rad59Δ* and *rad52Δ* mutants on MMEJ frequency (Table 1), which supports a Rad51-dependent inhibition by Rad52. Taken together, a Rad51-independent effect of Rad52 in annealing MHs during MMEJ is not supported by our data, but we cannot rule out a supportive effect of Rad52 on MMEJ using MHs shorter than 16 bp.

The key finding reported here is a direct role of DNA polymerase δ in MMEJ. Our understanding of the identity of the DNA polymerases involved in MMEJ is incomplete. In *Drosophila melanogaster*, DNA polymerase theta was shown to be critical for Alt-EJ (74). However, budding yeast does not contain a homolog for this DNA polymerase (75). In *S. cerevisiae*, MMEJ seems to be dependent on Pol32, and a role of Rev3 has been excluded (10). Our results demonstrate directly that Pol δ is required for DSB repair using MMEJ, which is largely independent of MH length and sequence continuity. First, consistent with previous results, we observed a significant decrease in the repair frequency of DSBs using varying lengths of MH with mismatches in *pol32Δ* mutants (Fig. 3*A*). Furthermore, a decrease of over 170-fold occurred in *pol32Δ* mutants when the MH without mismatches (20 bp) was used for repair, suggesting Pol32 becomes critical for MMEJ when the MH has no mismatches. Second, we demonstrate a similar decrease in MMEJ repair in *pol3-ct* mutants affecting the catalytic subunit of Pol δ, suggesting the function Pol32 in the Pol δ holoenzyme, as opposed to alternative complexes containing Pol32, affects MMEJ (Fig. 3*B*). The difference in the specific effects on the different MMEJ substrates in *pol32* and *pol3-ct* mutants raises the possibility of a more complex situation involving multiple polymerases in a single MMEJ event, consistent with the small but significant effect of *rev3Δ* mutants on certain MMEJ substrates. Third, we made use of a proofreading-deficient *pol3-01* mutant to show that Pol δ directly accesses the 3′-OH end during the DNA synthesis step in MMEJ and can act on proximal mismatches (Fig. 3 *C* and *D*). Fourth, we provide physical evidence by ChIP that Pol3 directly associates with DSBs showing kinetics that are consistent with a role in the DNA synthesis step of MMEJ. The maximum enrichment of *his3-Δ3′* at 6 h occurs 2 h after repression of HO endonuclease expression and thus DSB formation. Furthermore, the continued association of Pol3 with *his3-Δ3′* at 8 h suggests the repair process using MHs is slow and takes longer to complete than HR-mediated DSB repair (55, 76, 77). Finally, we demonstrate the association of Pol3 with the DSB is largely dependent on the activity of the Rad1–Rad10 heterodimer, as the enrichment of *his3-Δ3′* is reduced up to fivefold in *rad1Δ/rad1Δ* mutants compared with cells with functional Rad1. This observation is further supported by the genetic dependence of MMEJ on Rad1 in His^+ recombinant formation.

The involvement of Pol δ in MMEJ prompted us to examine other DNA polymerases involved in DSB repair using MHs. An early study in MMEJ by the Lee laboratory showed a modest role of Pol λ in MMEJ (5), which is supported by in vivo evidence showing Pol λ is proficient in gap filling of annealed MHs (38, 42). Consistent with the above results, we observed a decrease in the MMEJ frequency of *pol4Δ/pol4Δ* mutants and early association of Pol λ with MMEJ repair substrates. The synergistic decrease in *pol4Δ/pol4Δ pol32Δ/pol32Δ* and *pol4Δ/pol4Δ pol3-ct/pol3-ct* double mutants suggests dynamic, mutually dependent roles for Pol λ and Pol δ in promoting MMEJ. These results are a departure from a previous report examining *pol4Δ pol32Δ* double mutants (5), which show no difference between the single and double mutants. This difference is potentially due to several factors, which includes the acute expression of HO endonuclease, strain differences, use of diploid strains, longer MHs, and longer nonhomologous flaps in our study. One possibility is Pol λ and Pol δ function in separate pathways to promote MMEJ, with Pol δ-dependent repair contributing more to the overall number of MMEJ recombinants. Alternatively, Pol λ and Pol δ could function in the same pathway and cooperate in the repair process. We favor the latter explanation. Pol λ is proficient at extension in the absence of PCNA, lacks proofreading, and can extend even when the 3′-hydroxyl end contains a mismatch (42). These properties may endow Pol λ with greater efficiency than Pol δ, which requires PCNA and proofreads, at extending specific, possibly transient, heteroduplex molecules, which have low thermostability. The ChIP data show interdependence of the Pol λ and Pol δ association with the break site, not allowing a clear conclusion about a possible temporal sequence of action between both polymerases. The early Pol4 association with the DSB MMEJ substrate is reduced in *pol3-ct* mutants, and the partial dependence of the Pol3 association with the DSB substrate at 4 and 6 h suggests a more dynamic interaction during MMEJ, which is consistent with a two-polymerase model. This interaction is supported by previous results demonstrating the cooperation between Pol4 and Pol3 in gap filling during the repair of broken plasmids (78). A two-polymerase model has been proposed for lesion bypass of DNA damage in yeast and mammalian cells (79, 80) and similarly may allow for the most efficient polymerase to function during the initial and subsequent extension of MMEJ intermediates.

The importance of MMEJ has been highlighted by recent reports of MH use in various cellular repair processes and the presence of MH at chromosomal breakpoints (6, 81–83). However, whether alt-EJ represents a distinct repair pathway in mammalian cells and its role in cancer development is under debate (84). One potential problem is alt-EJ being defined as any DSB repair event independent of the Ku70–Ku80 heterodimer. These events are often associated with large deletions, insertions, and either no MHs or MHs ranging from 1 to 25 nt (85), but they may not all represent the same pathway for repair. It has been proposed that the repair junctions featuring limited or no MHs were repaired by a NHEJ pathway using alternative components to substitute for the canonical NHEJ components (84). Although the use of alternative NHEJ components could affect repair efficiency and the types of junctions formed, it does not explain the use of longer MHs, which are used at similar frequencies in both NHEJ-deficient and NHEJ-proficient cells (10, 37, 85). Examination of MH use in mammalian cells and yeast shows a similar range of 5–22 nt used for repair, but the frequency of repair appears to be higher in mammalian cells compared with yeast (4, 10, 21, 37, 86–88). We favor a model where longer MHs, such as those used in this study, are revealed following resection and form a stable base pairing relationship, which is further stabilized by DNA polymerase extension of the repair intermediate. Perhaps the rate-limiting step in the repair of DSBs using MHs is the formation and stability of the pairing intermediate and subsequent extension of the 3′-hydroxyl end by a DNA polymerase. Therefore, a DSB not repaired by NHEJ using limited or no MHs is subject to resection and repair by HR or MMEJ depending on the length of homology and the availability of the repair proteins.

Materials and Methods

Strain and Plasmid Construction. All yeast strains used in this study were isogenic with W303-1A but were wild type at the *RAD5* locus (Table S3). The *rad52::TRP1*, *ku70::TRP1*, *rad1::LEU2*, *rad51::LEU2*, and *pol3*-01 mutants were kindly provided by A. Bailis, Beckman Research Institute of the City of Hope, Duarte, CA (55, 89, 90). The *pol32::KANMX* and *pol3-ct* mutants were a generous gift from L. Symington, Columbia University, New York, (91) and L. Maloisel, Commissariat à l'énergie atomique et aux énergies alternatives, Fontenay-aux-Roses, France (48), respectively. The *pol4::KANMX* mutant was generated by PCR amplification of *KANMX* using pWDH517 as a template. The primers contain 50 nucleotides on their 5′ end, which share homology to sequences upstream and downstream of the *POL4* ORF. The deletion of the *POL4* ORF was verified by PCR in the transformant. Because the *pol3-01* is a mutator allele, all diploid strains with this mutation were constructed from haploid strains derived from freshly sporulated heterozygous diploid strains (see Table S3). The *pol3-ct* and *pol3-01* genotypes were determined by PCR and DNA sequencing.

The *his3-Δ3′-HOcs* MMEJ substrate cassettes were generated by PCR from the fusion of two smaller PCR fragments into a single larger *his3-Δ3′-HOcs* fragment. Using pLAY500 (55) as a template, an 810 bp fragment was amplified using a primer (olWDH946; sequences for all oligonucleotides are listed in Table S4) complementary to nucleotides upstream of the *HIS3* coding sequence and another corresponding to nucleotides 294–318 within the *HIS3* coding sequence (ol1659, 14-**2**-2 bp; ol1657, 14-**2**-4 bp; ol1661, 14-**2**-9 bp; ol1128, 16 bp; ol1074, 20 bp; ol1129, 25 bp). A second 600 bp fragment was amplified from pLAY500 using a primer complementary to the 5′ end of the 117 bp HOcs plus varying MHs complementary to nucleotides 294–318 of the *HIS3* coding sequence (ol1660, 14-**2**-2 bp; ol1658, 14-**2**-4 bp; ol1662, 14-**2**-9 bp; ol1130, 16 bp; ol1075, 20 bp; ol1131, 25 bp) and another primer complementary to nucleotides downstream of the *HIS3* coding sequence (ol949). The shared MH between the 810 bp and 600 bp PCR fragments was modified to create all of the various MHs used in this study (14-**2**-2 bp, 14-**2**-4 bp, 14-**2**-9 bp, 16 bp, and 25 bp). The 810 bp and 600 bp PCR fragments corresponding to each of the above MHs were paired and used as templates to amplify a larger fragment of *his3-Δ3′-HOcs*, each with a defined MH length and sequence continuity. The *his3-Δ3′-HOcs* fragments were digested with BamHI and cloned into YIp365R, which possesses a *URA3*-selectable marker that had been digested with BamHI. Each YIp365R+ *his3-Δ3′-HOcs* was linearized by digestion with *Msc*I to target its transplacement into the *HIS3* locus following transformation and selection for uracil prototrophy. Uracil prototrophs were plated to 5-FOA media to select for plasmid loss, and the resulting 5-FOA^r colonies assessed for integration by PCR and sequencing.

Construction of the other translocation assay components *his3-Δ200*, *leu2::HOcs-his3-Δ5′$_{(300)}$*, and *trp1::GAL1-HO-KAN-MX* were published previously (55). All strains possess the *his3-Δ5′* substrate at the *LEU2* locus on one copy of chromosome III. The *his3-Δ3′* substrates are located at the *HIS3* locus on one copy of chromosome XV. The *his3-Δ5′* and *his3-Δ3′* substrates share varying amounts of MH (14-**2**-2 bp, 14-**2**-4 bp, 14-**2**-9 bp, 16 bp, 20 bp, and 25 bp) within the *HIS3* coding sequence.

Interchromosomal MMEJ Assay and Analysis. We inoculated 2 mL cultures of YP-Raffinose medium containing 1% yeast extract, 2% (wt/vol) peptone, and 2% (wt/vol) raffinose with single colonies and incubated them for 24 h at 30 °C. The next day, galactose was added to the cultures to a final concentration of 2% (vol/vol) to induce expression of the HO endonuclease. After 4 h of induction, the cells were plated to medium lacking histidine, and the interchromosomal MMEJ frequency was determined by dividing the number of histidine prototrophic colonies by the total number of viable cells as determined by plating dilutions onto YPD. The median translocation frequencies represent at least 20 independent cultures, and the 95% confidence intervals were determined using Table S5. Selected YPD and His$^+$ recombinant colonies from substrates using the 14-**2**-4 bp of MH for repair were subjected to PCR amplification of the MMEJ product (ol968 and ol1013), reciprocal translocation (ol936 and ol1549), *leu2-3,112* (ol936 and ol1623), *MATa* (olAP53 and olAP54), *MATα* (olAP52 and olAP54), *his3Δ3′* (ol1013 and ol1549), and *his3Δ5′* (ol953 and ol936) loci. Subsequent analysis of the MMEJ PCR product by sequencing and restriction digestion was used to determine which two nucleotides within the mismatched MH were retained. Analysis of DSB formation by HO endonulcease, following the addition of galactose, was done using quantitative PCR (qPCR) with primers flanking the 117 bp HO recognition sequence located adjacent to the *his3Δ3′* allele (ol935 and ol960). The qPCR signal was normalized to the PCR amplification signal from *SAM1*, which is not located near any DSB and the percent of broken molecules at the 0 h time point.

Cell Viability. Cell viability was determined from YP-Raffinose cultures of the indicated genotypes with the 14-**2**-4 bp substrate after the addition of galactose. HO endonuclease was induced for 4 h at 30 °C, at which point the cell number was assessed by hemocytometer. Approximately 200–500 galactose-treated cells were plated to YPD, incubated at 30 °C for 4 d, and the number of colonies counted. Cell viability was determined by dividing the number of colonies by the number of cells plated and multiplying the quotient by 100. The mean plating efficiencies from at least 10 independent trials ± SEM were reported. Differences between plating efficiencies for which the ±SEM did not overlap are considered significantly different.

ChIP Assay. Newly dissected mutant spores of *rad52::TRP1*, *pol4::KANMX rad52::TRP1 pol3-ct rad52::TRP1*, and *rad1::LEU2 rad52::TRP1* double mutants possessing the interchromosomal MMEJ substrates, which share 14-**2**-4 bp of MH, were grown in YPD overnight, diluted to an OD_{600} of 0.2 in fresh YP-Raffinose, and allowed to grow to an OD_{600} of ∼1.0, at which time 45 mL was removed (0 h), pelleted, and immediately subject to the ChIP procedure described previously (56). Galactose was added to the remaining culture to a final concentration of 2% (vol/vol), which induces the expression of HO endonuclease and DSB formation at the *his3Δ3′* allele. At varying intervals following the addition of galactose, 45 mL were removed and immediately subject to the ChIP procedure.

Briefly, the pelleted cells were exposed to formaldehyde, washed, lysed in a buffer containing protease inhibitors, and the DNA sheared to ∼500 bp by sonication. The whole cell extract was subjected to immunoprecipitation by incubating with 5 μL of Pol3 antiserum, kindly provided by Burgers, at 4 °C overnight with shaking. The next day, protein A agarose beads were added to the samples and incubated at 4 °C for 3 h. The beads were then washed successively in SDS, high salt, and LiCl solutions, and finally TE buffer. DNA/protein/antibody complexes were eluted from the beads with elution buffer (1% SDS/TE) and the DNA/protein cross-links reversed by incubation at 65 °C overnight. Proteins were then digested with proteinase K for 2 h, extracted with phenol: chloroform, and the DNA precipitated with ethanol. Selected DNA sequences were analyzed by qPCR in triplicate using a Roche LightCycler480 with the following primer sets: A 198 bp *SAM1* sequence was amplified with the primers ol1653 and ol1654 and a 166 bp sequence specific to the 5′ end of *HIS3* amplified with the primers ol1651 and ol1652. Relative quantification of the PCR products was performed using the Roche LightCycler480 software. The *HIS3* and *SAM1* PCR signals obtained by ChIP were normalized to *HIS3* and *SAM1* PCR signals obtained from the above ChIP strain inputs that have not been exposed to the Pol3 antibody. The normalized *HIS3* and *SAM1* PCR signals were used to obtain the H/S ratios. The mean H/S ratios ± 1 SEM reported were derived from two independent strains for each genotype and repeated a minimum of four times. The *SAM1* PCR was chosen as the control locus for the *HIS3* PCR because it is not located near an induced DSB sequence.

ACKNOWLEDGMENTS. We thank Aurèle Piazza, Jie Liu, Sucheta Mukherjee, and William Wright for helpful discussions and comments on the manuscript and Adam Bailis, Lorraine Symington, and Laurent Maloisel for providing strains. We are grateful to Peter Burgers for providing antiserum (with support from NIH Grant GM32431) and William Knight for allowing us to reproduce Table S5. D.M. was partially supported by California Breast Cancer Research Program (CBCRP) Fellowship 15IB-0109 and Training Grant in Oncogenic Signals and Chromosome Biology CA108459. B.X.H.F. had partial support from a Presidential Undergraduate Fellowship from the University of California. This work was supported by NIH Grant GM58015 (to W.-D.H.).

1. Li X, Heyer WD (2008) Homologous recombination in DNA repair and DNA damage tolerance. *Cell Res* 18(1):99–113.
2. Bennardo N, Cheng A, Huang N, Stark JM (2008) Alternative-NHEJ is a mechanistically distinct pathway of mammalian chromosome break repair. *PLoS Genet* 4(6):e1000110.
3. Ma JL, Kim EM, Haber JE, Lee SE (2003) Yeast Mre11 and Rad1 proteins define a Ku-independent mechanism to repair double-strand breaks lacking overlapping end sequences. *Mol Cell Biol* 23(23):8820–8828.
4. Decottignies A (2007) Microhomology-mediated end joining in fission yeast is repressed by pku70 and relies on genes involved in homologous recombination. *Genetics* 176(3):1403–1415.
5. Lee K, Lee SE (2007) *Saccharomyces cerevisiae* Sae2- and Tel1-dependent single-strand DNA formation at DNA break promotes microhomology-mediated end joining. *Genetics* 176(4):2003–2014.
6. McVey M, Lee SE (2008) MMEJ repair of double-strand breaks (director's cut): Deleted sequences and alternative endings. *Trends Genet* 24(11):529–538.
7. Boboila C, Alt FW, Schwer B (2012) Classical and alternative end-joining pathways for repair of lymphocyte-specific and general DNA double-strand breaks. *Adv Immunol* 116:1–49.
8. Kidd JM, et al. (2010) A human genome structural variation sequencing resource reveals insights into mutational mechanisms. *Cell* 143(5):837–847.
9. Conrad DF, et al. (2010) Mutation spectrum revealed by breakpoint sequencing of human germline CNVs. *Nat Genet* 42(5):385–391.

10. Villarreal DD, et al. (2012) Microhomology directs diverse DNA break repair pathways and chromosomal translocations. *PLoS Genet* 8(11):e1003026.
11. Shin KH, et al. (2006) Abnormal DNA end-joining activity in human head and neck cancer. *Int J Mol Med* 17(5):917–924.
12. Zhang Y, Jasin M (2011) An essential role for CtIP in chromosomal translocation formation through an alternative end-joining pathway. *Nat Struct Mol Biol* 18(1):80–84.
13. Britten RJ, Kohne DE (1968) Repeated sequences in DNA. Hundreds of thousands of copies of DNA sequences have been incorporated into the genomes of higher organisms. *Science* 161(841):529–540.
14. Rothstein R, Helms C, Rosenberg N (1987) Concerted deletions and inversions are caused by mitotic recombination between delta sequences in *Saccharomyces cerevisiae*. *Mol Cell Biol* 7(3):1198–1207.
15. Szankasi P, et al. (1986) Mitotic recombination between dispersed but related tRNA genes of *S. pombe* generates a reciprocal translocation. *Mol Gen Genet* 202(3):394–402.
16. de Koning AP, Gu W, Castoe TA, Batzer MA, Pollock DD (2011) Repetitive elements may comprise over two-thirds of the human genome. *PLoS Genet* 7(12):e1002384.
17. Strout MP, Marcucci G, Bloomfield CD, Caligiuri MA (1998) The partial tandem duplication of ALL1 (MLL) is consistently generated by Alu-mediated homologous recombination in acute myeloid leukemia. *Proc Natl Acad Sci USA* 95(5):2390–2395.
18. Nakaya SM, Hsu TC, Geraghty SJ, Manco-Johnson MJ, Thompson AR (2004) Severe hemophilia A due to a 1.3 kb factor VIII gene deletion including exon 24: Homologous recombination between 41 bp within an Alu repeat sequence in introns 23 and 24. *J Thromb Haemost* 2(11):1941–1945.
19. Zhang F, Gu W, Hurles ME, Lupski JR (2009) Copy number variation in human health, disease, and evolution. *Annu Rev Genomics Hum Genet* 10:451–481.
20. Argueso JL, et al. (2008) Double-strand breaks associated with repetitive DNA can reshape the genome. *Proc Natl Acad Sci USA* 105(33):11845–11850.
21. Truong LN, et al. (2013) Microhomology-mediated end joining and homologous recombination share the initial end resection step to repair DNA double-strand breaks in mammalian cells. *Proc Natl Acad Sci USA* 110(19):7720–7725.
22. Lee-Theilen M, Matthews AJ, Kelly D, Zheng S, Chaudhuri J (2011) CtIP promotes microhomology-mediated alternative end joining during class-switch recombination. *Nat Struct Mol Biol* 18(1):75–79.
23. Chiarle R, et al. (2011) Genome-wide translocation sequencing reveals mechanisms of chromosome breaks and rearrangements in B cells. *Cell* 147(1):107–119.
24. Simsek D, Jasin M (2010) Alternative end-joining is suppressed by the canonical NHEJ component Xrcc4-ligase IV during chromosomal translocation formation. *Nat Struct Mol Biol* 17(4):410–416.
25. Ferguson DO, et al. (2000) The nonhomologous end-joining pathway of DNA repair is required for genomic stability and the suppression of translocations. *Proc Natl Acad Sci USA* 97(12):6630–6633.
26. Zhu C, et al. (2002) Unrepaired DNA breaks in p53-deficient cells lead to oncogenic gene amplification subsequent to translocations. *Cell* 109(7):811–821.
27. Difilippantonio MJ, et al. (2000) DNA repair protein Ku80 suppresses chromosomal aberrations and malignant transformation. *Nature* 404(6777):510–514.
28. Wang JH, et al. (2008) Oncogenic transformation in the absence of Xrcc4 targets peripheral B cells that have undergone editing and switching. *J Exp Med* 205(13):3079–3090.
29. Bentley J, Diggle CP, Harnden P, Knowles MA, Kiltie AE (2004) DNA double strand break repair in human bladder cancer is error prone and involves microhomology-associated end-joining. *Nucleic Acids Res* 32(17):5249–5259.
30. Zhang Y, Rowley JD (2006) Chromatin structural elements and chromosomal translocations in leukemia. *DNA Repair (Amst)* 5(9-10):1282–1297.
31. Mattarucchi E, et al. (2008) Microhomologies and interspersed repeat elements at genomic breakpoints in chronic myeloid leukemia. *Genes Chromosomes Cancer* 47(7):625–632.
32. Edwards SL, et al. (2008) Resistance to therapy caused by intragenic deletion in BRCA2. *Nature* 451(7182):1111–1115.
33. Magnani C, et al. (1996) Short direct repeats at the breakpoints of a novel large deletion in the CFTR gene suggest a likely slipped mispairing mechanism. *Hum Genet* 98(1):102–108.
34. Luzi P, Rafi MA, Wenger DA (1995) Characterization of the large deletion in the GALC gene found in patients with Krabbe disease. *Hum Mol Genet* 4(12):2335–2338.
35. Canning S, Dryja TP (1989) Short, direct repeats at the breakpoints of deletions of the retinoblastoma gene. *Proc Natl Acad Sci USA* 86(13):5044–5048.
36. Windhofer F, Krause S, Hader C, Schulz WA, Florl AR (2008) Distinctive differences in DNA double-strand break repair between normal urothelial and urothelial carcinoma cells. *Mutat Res* 638(1-2):56–65.
37. Deng SK, Gibb B, de Almeida MJ, Greene EC, Symington LS (2014) RPA antagonizes microhomology-mediated repair of DNA double-strand breaks. *Nat Struct Mol Biol* 21(4):405–412.
38. Daley JM, Wilson TE (2005) Rejoining of DNA double-strand breaks as a function of overhang length. *Mol Cell Biol* 25(3):896–906.
39. Yu AM, McVey M (2010) Synthesis-dependent microhomology-mediated end joining accounts for multiple types of repair junctions. *Nucleic Acids Res* 38(17):5706–5717.
40. Hicks WM, Kim M, Haber JE (2010) Increased mutagenesis and unique mutation signature associated with mitotic gene conversion. *Science* 329(5987):82–85.
41. Payen C, Koszul R, Dujon B, Fischer G (2008) Segmental duplications arise from Pol32-dependent repair of broken forks through two alternative replication-based mechanisms. *PLoS Genet* 4(9):e1000175.
42. Wilson TE, Lieber MR (1999) Efficient processing of DNA ends during yeast nonhomologous end joining. Evidence for a DNA polymerase beta (Pol4)-dependent pathway. *J Biol Chem* 274(33):23599–23609.
43. Tseng HM, Tomkinson AE (2002) A physical and functional interaction between yeast Pol4 and Dnl4-Lif1 links DNA synthesis and ligation in nonhomologous end joining. *J Biol Chem* 277(47):45630–45637.
44. Pardo B, Ma E, Marcand S (2006) Mismatch tolerance by DNA polymerase Pol4 in the course of nonhomologous end joining in *Saccharomyces cerevisiae*. *Genetics* 172(4):2689–2694.
45. Capp JP, et al. (2006) The DNA polymerase lambda is required for the repair of non-compatible DNA double strand breaks by NHEJ in mammalian cells. *Nucleic Acids Res* 34(10):2998–3007.
46. Garcia-Diaz M, et al. (2005) Structure-function studies of DNA polymerase lambda. *DNA Repair (Amst)* 4(12):1358–1367.
47. Sneeden JL, Grossi SM, Tappin I, Hurwitz J, Heyer WD (2013) Reconstitution of recombination-associated DNA synthesis with human proteins. *Nucleic Acids Res* 41(9):4913–4925.
48. Maloisel L, Fabre F, Gangloff S (2008) DNA polymerase delta is preferentially recruited during homologous recombination to promote heteroduplex DNA extension. *Mol Cell Biol* 28(4):1373–1382.
49. Giot L, Chanet R, Simon M, Facca C, Faye G (1997) Involvement of the yeast DNA polymerase delta in DNA repair in vivo. *Genetics* 146(4):1239–1251.
50. Li X, Stith CM, Burgers PM, Heyer WD (2009) PCNA is required for initiation of recombination-associated DNA synthesis by DNA polymerase delta. *Mol Cell* 36(4):704–713.
51. Makarova AV, Stodola JL, Burgers PM (2012) A four-subunit DNA polymerase zeta complex containing Pol delta accessory subunits is essential for PCNA-mediated mutagenesis. *Nucleic Acids Res* 40(22):11618–11626.
52. Johnson RE, Prakash L, Prakash S (2012) Pol31 and Pol32 subunits of yeast DNA polymerase delta are also essential subunits of DNA polymerase zeta. *Proc Natl Acad Sci USA* 109(31):12455–12460.
53. Kurtzman CP, Fell JW (1998) *The Yeasts—A Taxonomic Study* (Elsevier, Amsterdam), 4th Ed, p 1076.
54. Haber JE (2012) Mating-type genes and MAT switching in *Saccharomyces cerevisiae*. *Genetics* 191(1):33–64.
55. Pannunzio NR, Manthey GM, Bailis AM (2008) RAD59 is required for efficient repair of simultaneous double-strand breaks resulting in translocations in *Saccharomyces cerevisiae*. *DNA Repair (Amst)* 7(5):788–800.
56. Meyer DH, Bailis AM (2008) Telomerase deficiency affects the formation of chromosomal translocations by homologous recombination in *Saccharomyces cerevisiae*. *PLoS One* 3(10):e3318.
57. Garg P, Burgers PM (2005) DNA polymerases that propagate the eukaryotic DNA replication fork. *Crit Rev Biochem Mol Biol* 40(2):115–128.
58. Burgers PM (2009) Polymerase dynamics at the eukaryotic DNA replication fork. *J Biol Chem* 284(7):4041–4045.
59. Nick McElhinny SA, Gordenin DA, Stith CM, Burgers PM, Kunkel TA (2008) Division of labor at the eukaryotic replication fork. *Mol Cell* 30(2):137–144.
60. Maloisel L, Bhargava J, Roeder GS (2004) A role for DNA polymerase delta in gene conversion and crossing over during meiosis in *Saccharomyces cerevisiae*. *Genetics* 167(3):1133–1142.
61. Smith CE, Lam AF, Symington LS (2009) Aberrant double-strand break repair resulting in half crossovers in mutants defective for Rad51 or the DNA polymerase delta complex. *Mol Cell Biol* 29(6):1432–1441.
62. Brocas C, Charbonnier JB, Dherin C, Gangloff S, Maloisel L (2010) Stable interactions between DNA polymerase delta catalytic and structural subunits are essential for efficient DNA repair. *DNA Repair (Amst)* 9(10):1098–1111.
63. Pâques F, Haber JE (1997) Two pathways for removal of nonhomologous DNA ends during double-strand break repair in *Saccharomyces cerevisiae*. *Mol Cell Biol* 17(11):6765–6771.
64. Jin YH, et al. (2005) The multiple biological roles of the 3′→5′ exonuclease of *Saccharomyces cerevisiae* DNA polymerase delta require switching between the polymerase and exonuclease domains. *Mol Cell Biol* 25(1):461–471.
65. Tran HT, Degtyareva NP, Gordenin DA, Resnick MA (1999) Genetic factors affecting the impact of DNA polymerase delta proofreading activity on mutation avoidance in yeast. *Genetics* 152(1):47–59.
66. Hicks WM, Yamaguchi M, Haber JE (2011) Real-time analysis of double-strand DNA break repair by homologous recombination. *Proc Natl Acad Sci USA* 108(8):3108–3115.
67. Symington LS, Rothstein R, Lisby M (2014) Mechanisms and regulation of mitotic recombination in *Saccharomyces cerevisiae*. *Genetics* 198(3):795–835.
68. Valencia M, et al. (2001) *NEJ1* controls non-homologous end joining in *Saccharomyces cerevisiae*. *Nature* 414(6864):666–669.
69. Frank-Vaillant M, Marcand S (2001) NHEJ regulation by mating type is exercised through a novel protein, Lif2p, essential to the ligase IV pathway. *Genes Dev* 15(22):3005–3012.
70. Kegel A, Sjostrand JO, Astrom SU (2001) Nej1p, a cell type-specific regulator of nonhomologous end joining in yeast. *Curr Biol* 11(20):1611–1617.
71. Heyer WD, Ehmsen KT, Liu J (2010) Regulation of homologous recombination in eukaryotes. *Annu Rev Genet* 44:113–139.
72. Mortensen UH, Bendixen C, Sunjevaric I, Rothstein R (1996) DNA strand annealing is promoted by the yeast Rad52 protein. *Proc Natl Acad Sci USA* 93(20):10729–10734.
73. Sugiyama T, New JH, Kowalczykowski SC (1998) DNA annealing by Rad52 protein is stimulated by specific interaction with the complex of replication protein A and single-stranded DNA. *Proc Natl Acad Sci USA* 95(11):6049–6054.
74. Chan SH, Yu AM, McVey M (2010) Dual roles for DNA polymerase theta in alternative end-joining repair of double-strand breaks in Drosophila. *PLoS Genet* 6(7):e1001005.
75. Burgers PM, et al. (2001) Eukaryotic DNA polymerases: Proposal for a revised nomenclature. *J Biol Chem* 276(47):43487–43490.
76. Aylon Y, Liefshitz B, Bitan-Banin G, Kupiec M (2003) Molecular dissection of mitotic recombination in the yeast *Saccharomyces cerevisiae*. *Mol Cell Biol* 23(4):1403–1417.
77. Yan CT, et al. (2007) IgH class switching and translocations use a robust non-classical end-joining pathway. *Nature* 449(7161):478–482.

78. Chan CY, Galli A, Schiestl RH (2008) Pol3 is involved in nonhomologous end-joining in *Saccharomyces cerevisiae*. *DNA Repair (Amst)* 7(7):1531–1541.
79. Prakash S, Prakash L (2002) Translesion DNA synthesis in eukaryotes: A one- or two-polymerase affair. *Genes Dev* 16(15):1872–1883.
80. Shachar S, et al. (2009) Two-polymerase mechanisms dictate error-free and error-prone translesion DNA synthesis in mammals. *EMBO J* 28(4):383–393.
81. Stephens PJ, et al. (2011) Massive genomic rearrangement acquired in a single catastrophic event during cancer development. *Cell* 144(1):27–40.
82. Liu P, Carvalho CM, Hastings PJ, Lupski JR (2012) Mechanisms for recurrent and complex human genomic rearrangements. *Curr Opin Genet Dev* 22(3):211–220.
83. Cortizas EM, et al. (2013) Alternative end-joining and classical nonhomologous end-joining pathways repair different types of double-strand breaks during class-switch recombination. *J Immunol* 191(11):5751–5763.
84. Pannunzio NR, Li S, Watanabe G, Lieber MR (2014) Non-homologous end joining often uses microhomology: Implications for alternative end joining. *DNA Repair (Amst)* 17:74–80.
85. Deriano L, Roth DB (2013) Modernizing the nonhomologous end-joining repertoire: Alternative and classical NHEJ share the stage. *Annu Rev Genet* 47:433–455.
86. Sharma S, et al. (2015) Homology and enzymatic requirements of microhomology-dependent alternative end joining. *Cell Death Dis* 6:e1697.
87. Truong LN, et al. (2014) Homologous recombination is a primary pathway to repair DNA double-strand breaks generated during DNA rereplication. *J Biol Chem* 289(42): 28910–28923.
88. Kabotyanski EB, Gomelsky L, Han JO, Stamato TD, Roth DB (1998) Double-strand break repair in Ku86- and XRCC4-deficient cells. *Nucleic Acids Res* 26(23):5333–5342.
89. Manthey GM, Bailis AM (2002) Multiple pathways promote short-sequence recombination in *Saccharomyces cerevisiae*. *Mol Cell Biol* 22(15):5347–5356.
90. Mito E, et al. (2008) Mutagenic and recombinagenic responses to defective DNA polymerase delta are facilitated by the Rev1 protein in pol3-t mutants of *Saccharomyces cerevisiae*. *Genetics* 179(4):1795–1806.
91. Ho CK, Mazon G, Lam AF, Symington LS (2010) Mus81 and Yen1 promote reciprocal exchange during mitotic recombination to maintain genome integrity in budding yeast. *Mol Cell* 40(6):988–1000.